inflammation.[3] LPS is frequently detected in the middle ear of patients with otitis media with effusion and induces the expression of inflammatory cytokines and mucosal inflammation in middle ear cavity.[9] The previous studies showed that LPS induced significant production of cytokines in mouse middle ear, and the maximum production of cytokines in middle ear cavity was seen at 24 hours after transtympanic injection with LPS.[10] The purpose of this study was to clarify the effects of GM-CSF in LPS-induced otitis media.

MATERIALS AND METHODS

Animals

C57BL/6 mice (6–12 weeks old) were used for this study. Mice were housed under specific pathogen-free conditions in the Department of Animal Resources at Okayama University. All animal studies were performed in accordance with the animal protection rules. All study procedures were approved by The Animal Research Control Committee of Okayama University. Otoscopic examination was performed for all mice before treatment to ensure that the tympanic membranes were normal and that no middle ear effusion was present. Mice were deeply anesthetized using intraperitoneal injection of both ketamine (100 mg/kg body weight) and xylazine (10 mg/kg body weight).

Expression of GM-CSF Induced by LPS

Experimental otitis media was induced by injection of LPS into the bilateral middle ear, as reported previously.[11] Mice were randomly allocated to an experimental group (n = 6) and a control group (n = 6) in each time point (3, 6, 12, and 24 hours). A total of 48 mice (96 ears) were used in this study. The experimental group received LPS (1.0 mg/mL; Sigma-Aldrich, St Louis, MO) via transtympanic injection using a 30-gauge needle. Phosphate-buffered saline (PBS) at 0.01 M was injected into the middle ear of animals in the control group. In either case, the middle ear and external ear canal were filled with 20 μL of LPS or PBS. Mice were sacrificed at 3, 6, 12, or 24 hours after injection of LPS or PBS. Middle ears were then washed transtympanically with 200 μL of PBS. The collected PBS from the middle ear wash was centrifuged. The supernatant was transferred to 1.5-mL microcentrifuge tubes (Treff AG, Degersheim, Switzerland) and stored at −30°C until analysis. Concentrations of GM-CSF in PBS collected from the middle ear wash were determined by enzyme-linked immunosorbent assay (ELISA) using a Mouse GM-CSF Quantikine ELISA Kit according to the instructions from the manufacturer (MGM00; R&D Systems, Minneapolis, MN).

Effect of Anti-GM-CSF in Experimental Otitis Media

C57BL/6 mice (6–12 weeks old) received transtympanic injection of 20 μL of LPS (1.0 mg/mL) or PBS. A total of 48 mice were used in this study (n = 6 in each subgroup). Two hours before transtympanic injection of LPS or PBS into the middle ear, mice received intraperitoneal injection of GM-CSF–neutralizing antibody (MAB415; R&D Systems) at different doses (30, 100, or 300 μg/animal) or control immunoglobulin (Ig) G_{2A} (MAB006, 300 μg/animal; R&D Systems). Because the previous studies showed that the maximum cytokine production was observed 24 hours after middle ear injection with LPS,[10] mice were sacrificed at 24 hours after transtympanic injection of LPS or PBS. Middle ears were washed with 500 μL of PBS. The collected PBS from the middle ear wash was centrifuged. The supernatant was stored at −30°C until analysis. Concentrations of macrophage inflammatory protein (MIP)-2, keratinocyte chemoattractant (KC), interleukin (IL)-1β, and tumor necrosis factor (TNF)-α were measured by ELISA kits in accordance with the instructions from the manufacturer (MIP-2, mouse CXCL2/MIP-2 DuoSet, R&D Systems; KC, Quantikine Mouse CXCL1/KC Immunoassay Set, R&D Systems; IL-1β, BD OptEIA Mouse IL-1β ELISA Set, BD Biosciences Pharmingen, San Diego, CA; TNF-α, BD OptEIA Mouse TNF (Mono/Mono) ELISA Set, BD Biosciences Pharmingen).

Histologic Examination

Temporal bones were removed immediately after sacrifice and processed for histologic examination. Bone specimens were placed in 4% paraformaldehyde for 48 hours and decalcified in 10% ethylenediaminetetraacetic acid for 3 weeks at 4°C. After dehydration, specimens were embedded in paraffin and sectioned at a thickness of 10 μm, then mounted on glass slides, processed using hematoxylin-and-eosin staining, and evaluated under light microscopy.

Statistical Analysis

Concentrations of GM-CSF, MIP-2, KC, IL-1β, and TNF-α are given as mean ± standard error of the mean. Statistical analyses were performed using nonparametric Mann-Whitney U tests. Significant differences were established at the level of $P < .05$.

RESULTS

Production of GM-CSF in the Middle Ear With LPS

We first examined GM-CSF production following LPS injection in experimental otitis media. Levels of GM-CSF protein were quantified using ELISA. Significant production of GM-CSF was detected 6 hours after transtympanic injection with LPS as compared with PBS ($P = .004$), followed by a decrease in its concentration at 24 hours (Fig. 1).

Role of GM-CSF in LPS-Induced Otitis Media

Because significant expression of GM-CSF was observed in the middle ear in LPS-injected mice, we

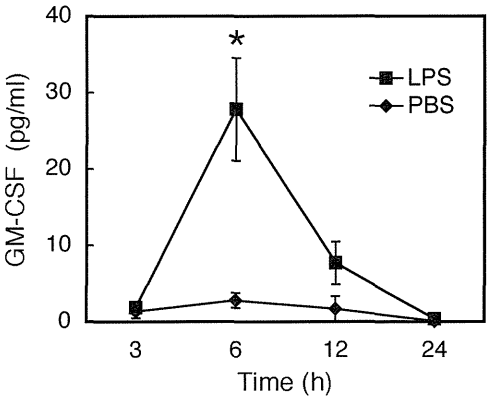

Fig. 1. Concentrations of granulocyte/macrophage colony–stimulating factor (GM-CSF) in middle ear effusion at 3, 6, 12, and 24 hours after transtympanic injection of lipopolysaccharide (LPS) (n = 6 [12 ears] in each time point) or phosphate-buffered saline (PBS) (n=6 [12 ears] in each time point). *$P < .05$.

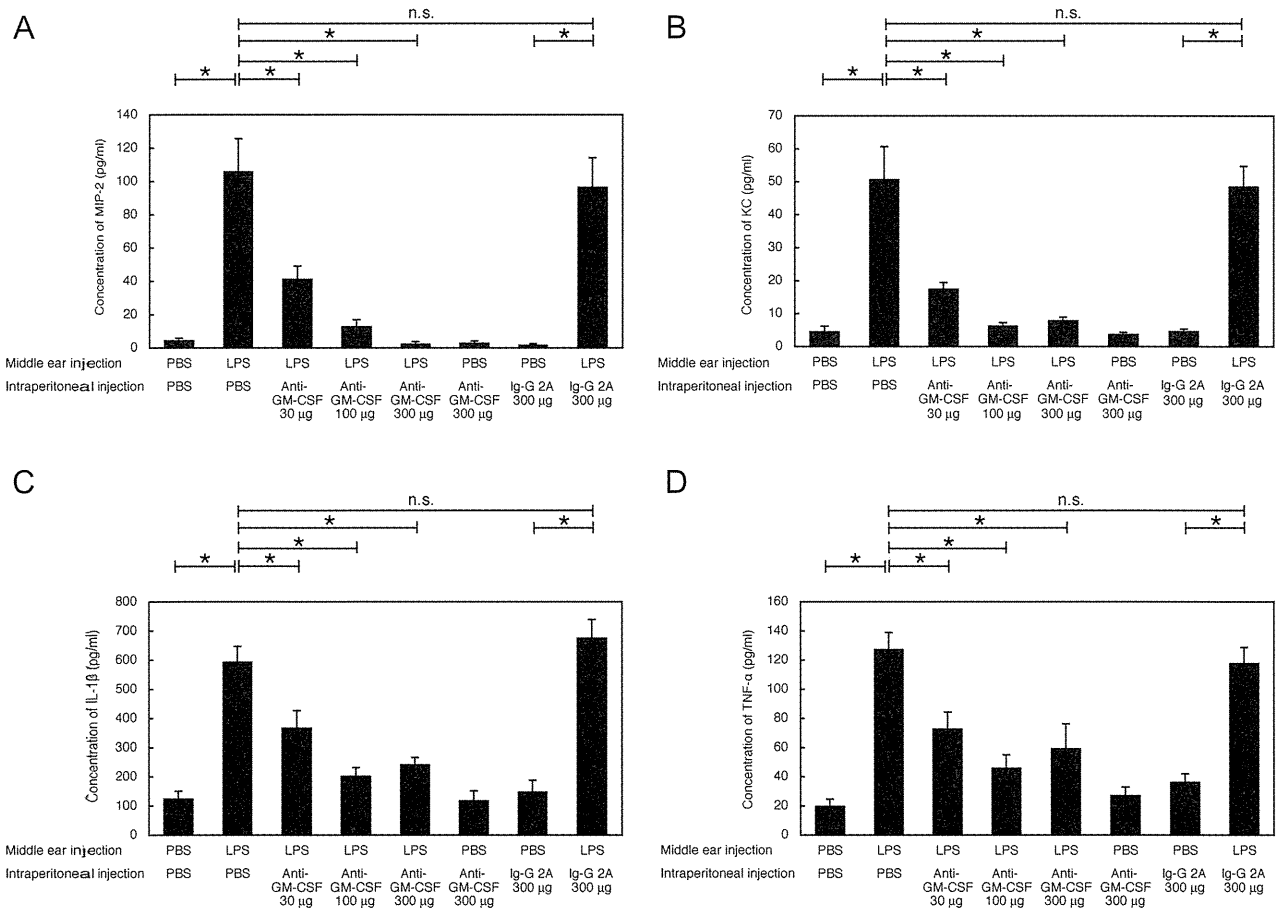

Fig. 2. Concentrations of macrophage inflammatory protein (MIP)-2 (A), keratinocyte chemoattractant (KC) (B), interleukin (IL)-1β (C), and tumor necrosis factor (TNF)-α (D) in middle ear effusion. Pretreatment with granulocyte/macrophage colony–stimulating factor (GM-CSF) neutralizing antibody via intraperitoneal injection significantly reduced the production of inflammatory mediators induced by lipopolysaccharide (LPS). Six mice (12 ears) were used in each group. Ig = immunoglobulin; n.s. = not significant; PBS = phosphate-buffered saline. *$P < .05$.

sought to determine the role of GM-CSF in middle ear inflammation. To clarify the effects of GM-CSF, we investigated whether neutralizing the bioactivity of endogenous GM-CSF using neutralizing antibody would affect levels of LPS-induced MIP-2, KC, IL-1β, and TNF-α secretion in the middle ear.

Figure 2A shows mean concentrations of MIP-2 in middle ear effusions at 24 hours after transtympanic administration of LPS or PBS. All mice were pretreated with PBS, GM-CSF–neutralizing antibody, or control IgG_{2A} intraperitoneally 2 hours before middle ear injection of LPS or PBS. In mice pretreated with PBS intraperitoneally, levels of MIP-2 in PBS-injected mice were low, and mean concentrations of MIP-2 were significantly higher in LPS-injected mice than in PBS-injected mice ($P < .001$). Pretreatment with GM-CSF–neutralizing antibody inhibited secretion of MIP-2 following middle ear injection of LPS in a dose-dependent manner. In mice pretreated with 300 μg per animal of GM-CSF–neutralizing antibody, no significant differences in levels of MIP-2 were identified between middle ear injection of LPS and PBS. Mice pretreated with control IgG_{2A} showed similar findings to PBS-pretreated mice in terms of the levels of MIP-2 following middle ear injection of LPS.

Mean concentrations of KC induced by middle ear injection of LPS or PBS are shown in Figure 2B. Middle ear injection of LPS induced significant production of KC as compared with middle ear injection of PBS. Intraperitoneal pretreatment with GM-CSF–neutralizing antibody suppressed the significant KC production induced by LPS in the mouse middle ear (30 μg/animal, $P = .011$; 100 μg/animal, $P < .001$; 300 μg/animal, $P < .001$). Mice pretreated with control IgG_{2A} showed similar findings to PBS-pretreated mice in terms of KC levels following middle ear injection of LPS or PBS.

Expressions of IL-1β induced by middle ear injection of LPS or PBS are shown in Figure 2C. In PBS-pretreated mice, LPS induced significant IL-1β secretion in the middle ear ($P < .001$). Concentrations of IL-1β induced by LPS in GM-CSF–neutralizing antibody-pretreated mice were significantly decreased as compared with levels in PBS-pretreated mice (30 μg/animal, $P = .007$; 100 μg/animal, $P < .001$; 300 μg/animal, $P < .001$). GM-CSF–neutralizing antibody pretreated mice (300 μg/animal) showed a significant difference between concentrations of IL-1β following middle ear injection of LPS or PBS ($P = .016$). Unlike MIP-2, IL-1β was not completely suppressed by GM-CSF–neutralizing antibody at 300 μg/animal.

Figure 2D shows the mean level of TNF-α. In mice pretreated intraperitoneally with PBS, concentrations of TNF-α were significantly higher following middle ear injection of LPS than after injection of PBS ($P < .001$). GM-CSF–neutralizing antibody inhibited LPS-induced secretion of TNF-α in the mouse middle ear (30 μg/animal, $P = .006$; 100 μg/animal, $P < .001$; 300 μg/animal, $P = .004$). In mice pretreated with 300 μg/animal of GM-CSF–neutralizing antibody, no significant difference was seen between TNF-α levels with LPS or PBS injection.

Histologic Findings

Histologic examination revealed that LPS induced severe infiltration of numerous inflammatory cells in the middle ear epithelium, and mucosal thickening was observed in the middle ear of mice inoculated with LPS into the middle ear (n = 6) (Fig. 3A). Middle ear effusion with neutrophils and monocytes/macrophages was observed in LPS-injected mice (Fig. 3A). In contrast, GM-CSF–neutralizing antibody pretreated mice showed reduced infiltration of inflammatory cells following middle ear injection of LPS (n = 6) (Fig. 3B). GM-CSF–neutralizing antibody pretreated mice had small amount of middle ear effusions with inflammatory cells. No middle ear effusion or mucosal inflammation was detected following middle ear injection of PBS in both PBS-pretreated mice (n = 6) (Fig. 3C) and mice pretreated with 300 μg/animal of neutralizing antibody (n = 6) (Fig. 3D).

DISCUSSION

The principle aim of the present study was to characterize the role of GM-CSF in otitis media with effusion. We used a mouse model of otitis media with effusion in this study. Administration of LPS alone into the middle ear cavity can induce otitis media with effusion in experimental animals.[12,13] Our findings in this study clearly showed that neutralization of endogenous GM-CSF by the neutralizing antibody significantly reduced infiltration of inflammatory cells and cytokine production in the middle ear of LPS-challenged mice.

Experimental animal studies have reported the therapeutic potential of neutralizing antibody for GM-CSF in lung inflammation.[14–16] Vlahos et al. showed that anti-GM-CSF treatment blocked cigarette smoke–

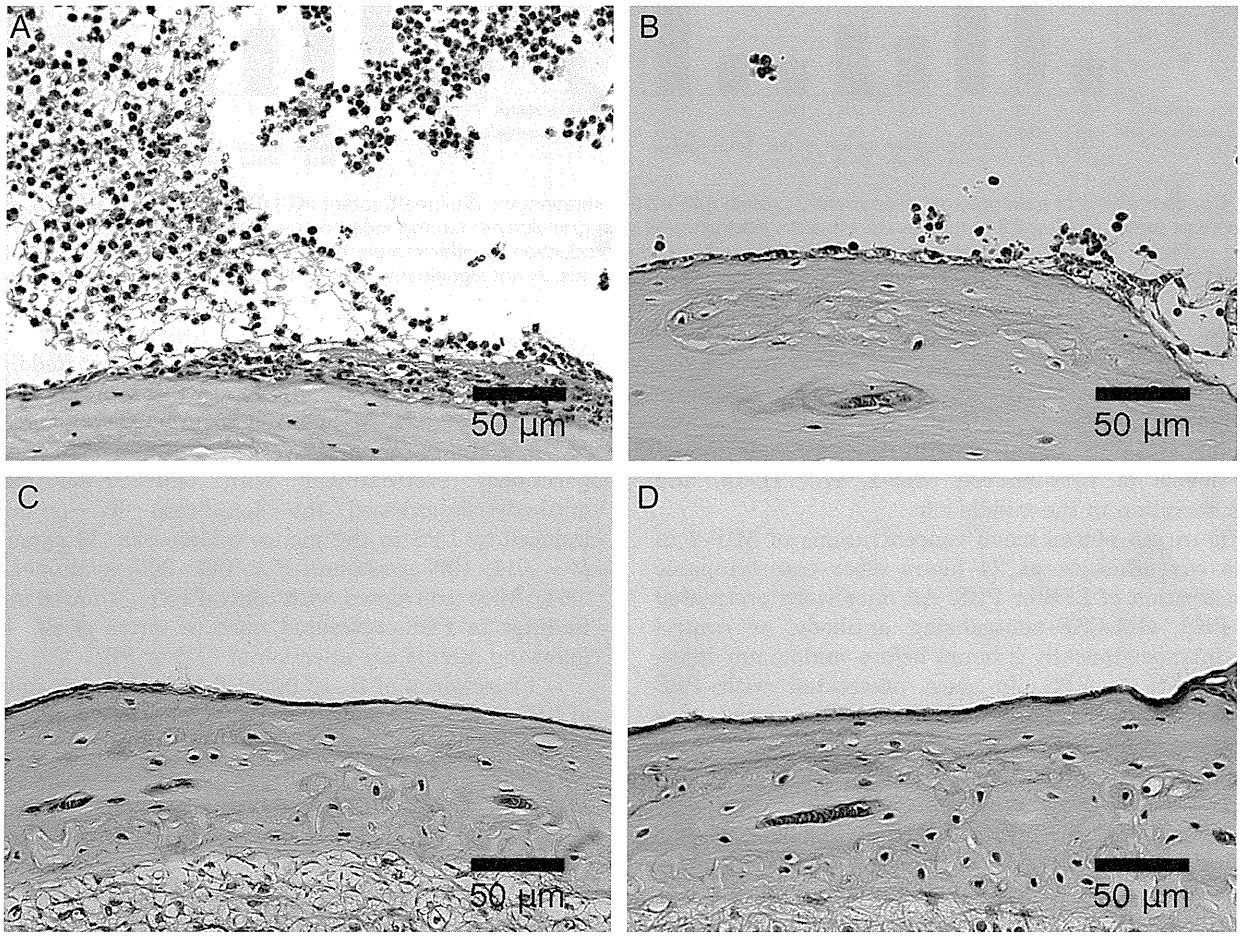

Fig. 3. Histologic findings in phosphate buffered saline (PBS)–pretreated mice (A) and granulocyte/macrophage colony–stimulating factor (GM-CSF) neutralizing antibody pretreated mice (B) with middle ear injection of lipopolysaccharide. Neutralization of GM-CSF was associated with reduced infiltration of inflammatory cells. In mice with middle ear injection of PBS, no evidence of inflammatory cell infiltration was observed in either PBS-pretreated mice (C) or GM-CSF–neutralizing antibody pretreated mice (D).

induced neutrophilia and macrophage accumulation in bronchoalveolar lavage fluid from mice.[15] Puljic et al. reported that pretreatment with GM-CSF neutralizing antibody inhibited the accumulation of neutrophils in a dose-dependent manner and reduced TNF-α and MIP-2 protein levels in bronchoalveolar lavage fluid from LPS-induced lung inflammation in mice.[14] This study showed that the production of IL-1β and KC, as well as TNF-α and MIP-2, following exposure to LPS was significantly suppressed by intraperitoneal injection of GM-CSF–neutralizing antibody.

Histologic examination in this study showed that LPS induced predominant infiltration of inflammatory cells, including neutrophils and monocytes/macrophages, into the middle ear epithelium of mice. We also showed that neutralization of GM-CSF dramatically reduced this mucosal inflammation induced by LPS. Pretreatment with intraperitoneal injection of control antibody (IgG_{2A}) had no significant effect. As both MIP-2 and KC are powerful chemokines capable of recruiting neutrophils in mice, the inhibition of neutrophil infiltration after treatment with anti-GM-CSF antibody may be a consequence of the reduced levels of MIP-2 and KC.

GM-CSF boosts IL-1β production by LPS in bone marrow–derived monocyte/macrophages and dendritic cells in mice.[17] The injection of GM-CSF in subcutaneous tissue enhances production of LPS-induced cytokines (TNF and IL-6) in mice.[18] The present study showed that LPS-induced IL-1β and TNF-α expressions were reduced, but not as dramatically suppressed as levels of MIP-2, by pretreatment with GM-CSF–neutralizing antibody. These findings suggest that the productions of IL-1β and TNF-α by LPS in the mouse middle ear are not solely dependent on the GM-CSF pathway.

Recombinant human TNF stimulates significant production of both messenger RNA and protein levels of GM-CSF in normal human lung fibroblasts.[19] The interaction between GM-CSF from airway epithelium and Th17 cells is important in promoting and sustaining neutrophilic inflammation, as observed in severe asthma and chronic obstructive pulmonary disease.[20] In addition, the significance of GM-CSF in the Th1/Th2/Th17 immune system has also been reported in autoimmune diseases.[21,22] Several antibody-based pharmacologic treatments using anti-CD20, anti-CD25, anti-IgE and anti-TNF antibodies are under development for malignant tumor, allergic disease, and rheumatoid arthritis. Anti-GM-CSF therapy might be a promising option for pulmonary inflammation induced by LPS.[14] The present study showed that treatment with GM-CSF–neutralizing antibody exerts significant effects on LPS-induced otitis media.

CONCLUSION

Systemic injection of GM-CSF–neutralizing antibody inhibits the middle ear inflammation induced by LPS in mice. Our findings suggest that GM-CSF may offer a novel therapeutic target for the management of intractable otitis media.

BIBLIOGRAPHY

1. Luong A, Roland PS. The link between allergic rhinitis and chronic otitis media with effusion in atopic patients. *Otolaryngol Clin North Am* 2008; 41:311–323.
2. Juhn SK, Jung MK, Hoffman MD, et al. The role of inflammatory mediators in the pathogenesis of otitis media and sequelae. *Clin Exp Otorhinolaryngol* 2008;1:117–138.
3. Leichtle A, Lai Y, Wollenberg B, Wasserman SI, Ryan AF. Innate signaling in otitis media: pathogenesis and recovery. *Curr Allergy Asthma Rep* 2011;11:78–84.
4. Smirnova MG, Birchall JP, Pearson JP. The immunoregulatory and allergy-associated cytokines in the aetiology of the otitis media with effusion. *Mediators Inflamm* 2004;13:75–88.
5. Hamilton JA. Colony-stimulating factors in inflammation and autoimmunity. *Nat Rev Immunol* 2008;8:533–544.
6. Yellon RF, Leonard G, Marucha PT, et al. Characterization of cytokines present in middle ear effusions. *Laryngoscope* 1991;101:165–169.
7. Himi T, Suzuki T, Kodama H, Takezawa H, Kataura A. Immunologic characteristics of cytokines in otitis media with effusion. *Ann Otol Rhinol Laryngol Suppl* 1992;157:21–25.
8. Smirnova MG, Birchall JP, Pearson JP. Evidence of T-helper cell 2 cytokine regulation of chronic otitis media with effusion. *Acta Otolaryngol* 2005;125:1043–1050.
9. Kariya S, Okano M, Aoji K, et al. Role of macrophage migration inhibitory factor in otitis media with effusion in adults. *Clin Diagn Lab Immunol* 2003;10:417–422.
10. Kariya S, Schachern PA, Cureoglu S, et al. Up-regulation of macrophage migration inhibitory factor induced by endotoxin in experimental otitis media with effusion in mice. *Acta Otolaryngol* 2008;128:750–755.
11. Eguchi M, Kariya S, Okano M, et al. Lipopolysaccharide induces proinflammatory cytokines and chemokines in experimental otitis media through the prostaglandin D2 receptor (DP)-dependent pathway. *Clin Exp Immunol* 2011;163:260–269.
12. DeMaria TF, Murwin DM. Tumor necrosis factor during experimental lipopolysaccharide-induced otitis media. *Laryngoscope* 1997;107:369–372.
13. Maeda K, Hirano T, Ichimiya I, Kurono Y, Suzuki M, Mogi G. Cytokine expression in experimental chronic otitis media with effusion in mice. *Laryngoscope* 2004;114:1967–1972.
14. Puljic R, Benediktus E, Plater-Zyberk C, et al. Lipopolysaccharide-induced lung inflammation is inhibited by neutralization of GM-CSF. *Eur J Pharmacol* 2007;557:230–235.
15. Vlahos R, Bozinovski S, Chan SP, et al. Neutralizing granulocyte/macrophage colony-stimulating factor inhibits cigarette smoke-induced lung inflammation. *Am J Respir Crit Care Med* 2010;182:34–40.
16. Vlahos R, Bozinovski S, Hamilton JA, Anderson GP. Therapeutic potential of treating chronic obstructive pulmonary disease (COPD) by neutralising granulocyte macrophage-colony stimulating factor (GM-CSF). *Pharmacol Ther* 2006;112:106–115.
17. Khameneh HJ, Isa SA, Min L, Nih FW, Ruedl C. GM-CSF signalling boosts dramatically IL-1 production. *PLoS One* 2011;6:e23025.
18. Brissette WH, Baker DA, Stam EJ, Umland JP, Griffiths RJ. GM-CSF rapidly primes mice for enhanced cytokine production in response to LPS and TNF. *Cytokine* 1995;7:291–295.
19. Munker R, Gasson J, Ogawa M, Koeffler HP. Recombinant human TNF induces production of granulocyte-monocyte colony-stimulating factor. *Nature* 1986;323:79–82.
20. Traves SL, Donnelly LE. Th17 cells in airway diseases. *Curr Mol Med* 2008;8:416–426.
21. Cornish AL, Campbell IK, McKenzie BS, Chatfield S, Wicks IP. G-CSF and GM-CSF as therapeutic targets in rheumatoid arthritis. *Nat Rev Rheumatol* 2009;5:554–559.
22. Codarri L, Gyulveszi G, Tosevski V, et al. RORγt drives production of the cytokine GM-CSF in helper T cells, which is essential for the effector phase of autoimmune neuroinflammation. *Nat Immunol* 2011;12:560–567.

好酸球性副鼻腔炎の病態と治療

岡野光博

キーワード●好酸球，喘息，外毒素，ロイコトリエン，鼻洗浄

はじめに

慢性副鼻腔炎に対する治療は1990年代以降に大きく変貌した．第1はマクロライド療法の普及である．特に感染性炎症に効果を示し，従来の薬物療法に比べ，手術適応となる患者の減少に貢献した．第2は内視鏡下副鼻腔手術（ESS）の進歩である．本手術は低侵襲であるのみならず，従来の経犬歯窩法に比較して有効性と安全性が飛躍的に向上した．しかしながら，症例を重ねるうちにこれらの治療に抵抗する難治例，すなわち難治性副鼻腔炎に遭遇するようになった．難治性副鼻腔炎は線毛機能不全などいくつかのフェノタイプに分けられるが，その代表が好酸球性副鼻腔炎（eosinophilic chronic rhinosinusitis）である．

I 好酸球性副鼻腔炎の臨床像

2002年，森山により好酸球性副鼻腔炎の臨床像が示された（表1）[1]．以後10年を越えるが，提唱された臨床像に大きな変更はなく，疾患概念は受容されている．

典型例は成人発症の副鼻腔炎で，両側性かつ多発性の浮腫状の鼻茸を示す．好酸球性副鼻腔炎のゆえんは鼻茸や副鼻腔粘膜に好酸球優位な炎症細胞浸潤がみられることである．また，上皮細胞の剝脱や分泌細胞の増加，基底膜の肥厚もみられる．ニカワ状の粘稠な分泌物の貯留を認め，粘液内にも好酸球浸潤がみられる（好酸球性ムチン）（図1）．中鼻甲介付近（中鼻道，嗅裂）付近の病変が強いため，早期より嗅覚障害を訴える．嗅覚障害を反映するように，上顎洞に比べ篩骨洞病変が優位であるが，進行すると汎副鼻腔病変となる．また，鼻茸のサイズに応じて鼻閉を訴える．喘息を合併することが多く，特にアスピリン喘息を合併する場合は難治である．アレルギー性鼻炎の関与は少なく，IgE値

表1　好酸球性副鼻腔炎の臨床像

- 成人，両側罹患で多発性の浮腫状の鼻茸
- 中鼻甲介付近（中鼻道，嗅裂）の病変が強く，下鼻甲介は所見が少ない．したがって嗅覚障害例が多い．
- 粘稠性分泌物（ニカワ状，多数の好酸球）の貯留
- 鼻アレルギー（I型）の関与が少なく，IgE値（特異，非特異）はさまざま
- 喘息（非アトピー），アスピリン喘息に伴うことが多い．
- 血中好酸球の増多，血中・鼻粘膜ECP濃度が高値
- 篩骨洞病変が中心であるが，汎副鼻腔病変例も多い．
- 上皮下に活性化好酸球浸潤，粘膜下の浮腫性変化，上皮細胞の剝脱と分泌細胞の増加
- 治療，特に手術治療に抵抗性（鼻茸の易再発，治癒不全例）
- ステロイド薬の全身投与が有効（局所ステロイド薬は無効）
- 喘息合併例では鼻粘膜の軽快・増悪は喘息の消長にほぼ一致

ECP；eosinophil cationic protein
（森山　寛：日本耳鼻咽喉科学会専門医通信2002；70：8-9より引用）

Pathogenesis and treatment of eosinophilic chronic rhinosinusitis

Mitsuhiro Okano：Department of Otolaryngology-Head and Neck Surgery, Okayama University Graduate School of Medicine, Dentistry and Pharmaceutical Sciences
岡山大学大学院医歯薬学総合研究科准教授（耳鼻咽喉・頭頸部外科学）

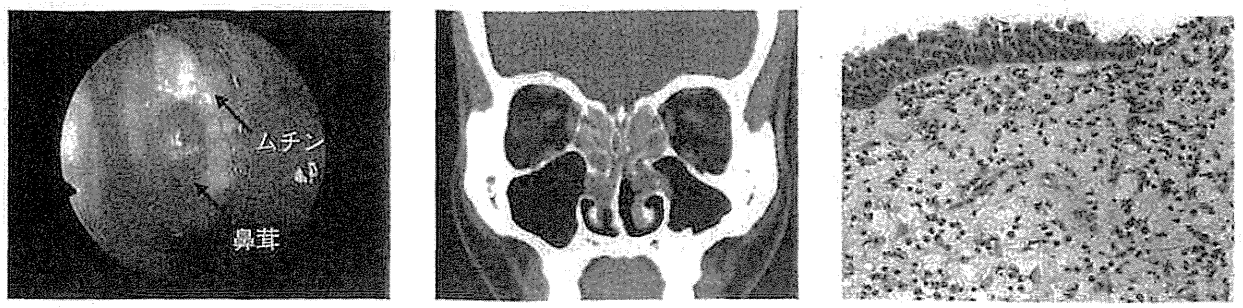

局所所見（右鼻腔）　CT所見　組織所見

図1　好酸球性副鼻腔炎の局所所見とCT所見と組織所見

はさまざまである．血中好酸球増多がみられることが多い．

マクロライド療法の効果は限定的ではあるが，ステロイド薬の全身投与にはよく反応する．病理像や病態が喘息と類似しており，好酸球性副鼻腔炎は，“上気道の喘息（asthma of the upper airway）”ともいわれる．

II 好酸球性副鼻腔炎の病態

好酸球性副鼻腔炎の増悪因子には，外的因子として黄色ブドウ球菌の菌体外毒素であるエンテロトキシン，真菌，ウイルスおよびバイオフィルムおよびTLRリガンドなどが，また内的因子としてアスピリン喘息合併例で示されるようにアラキドン酸代謝異常が疑われている．これらの因子により，上皮・バリア機能障害，あるいは自然免疫や獲得免疫の制御異常（dysregulation）が生じ，過剰な好酸球性炎症や鼻茸形成，ムチン産生などを来し，難治化に進むものと考えられている（**図2**）．

黄色ブドウ球菌エンテロトキシンはスーパー抗原として，あるいはアジュバントとして好酸球性炎症に関与する．マウスモデルでは，エンテロトキシンの経鼻的な曝露は好酸球性炎症を増悪する．鼻茸やムチン中にはエンテロトキシンや，エンテロトキシンに特異的なIgEが検出される[2]．エンテロトキシンは鼻茸を刺激し，好酸球性炎症に関わるサイトカイン・ケモカインであるIL-5，IL-13，RANTES産生を誘導する[3]．

鼻・副鼻腔における高い検出率から，副鼻腔炎の難治化に真菌が関与することも示唆されている[4]．鼻茸はアスペルギルスなどの真菌に反応し，有意なIL-5，IL-13，RANTES産生を示す．したがって，真菌への曝露は好酸球性副鼻腔炎の増悪因子となりうる[5]．一方，これらのサイトカインの産生量および産生比率はエンテロトキシンと比較して低い．慢性副鼻腔炎に対する抗真菌薬の効果に関して否定的な報告がみられることからも，好酸球性副鼻腔炎の病態における真菌の関与は限定的であるかもしれない．

アラキドン酸代謝異常も好酸球性炎症の重要な因子である．リポキシゲナーゼ(LO)系に注目すると，アスピリン喘息を合併した好酸球性副鼻腔炎患者の尿中ロイコトリエン濃度は有意に高く，ESSによって鼻茸を切除すると有意に低下する[6]．したがって，鼻茸は全身的にもロイコトリエン産生の重要な組織である．ロイコトリエン受容体のうち，鼻茸ではCysLT1受容体の発現が高く，浸潤好酸球数と正の相関を示す．

また，シクロオキシゲナーゼ（COX）系代謝に目を向けると，喘息患者，特にアスピリン喘息患者の鼻茸ではCOX-2発現が低い[7]．鼻茸のエンテロトキシンに対するサイトカイン産生はCOXを阻害することにより亢進する．この作用はアスピリン喘息の有無に関係なくみられることから，好酸球性副鼻腔炎の鼻茸は本質的にアスピリン不耐といえる．さらに，COX阻害の作用はPGE_2の添加により抑制されることから，内因性のPGE_2が好酸球性炎症に対して抑制的に働く[3]．グラム陰性菌由来のリポ多糖

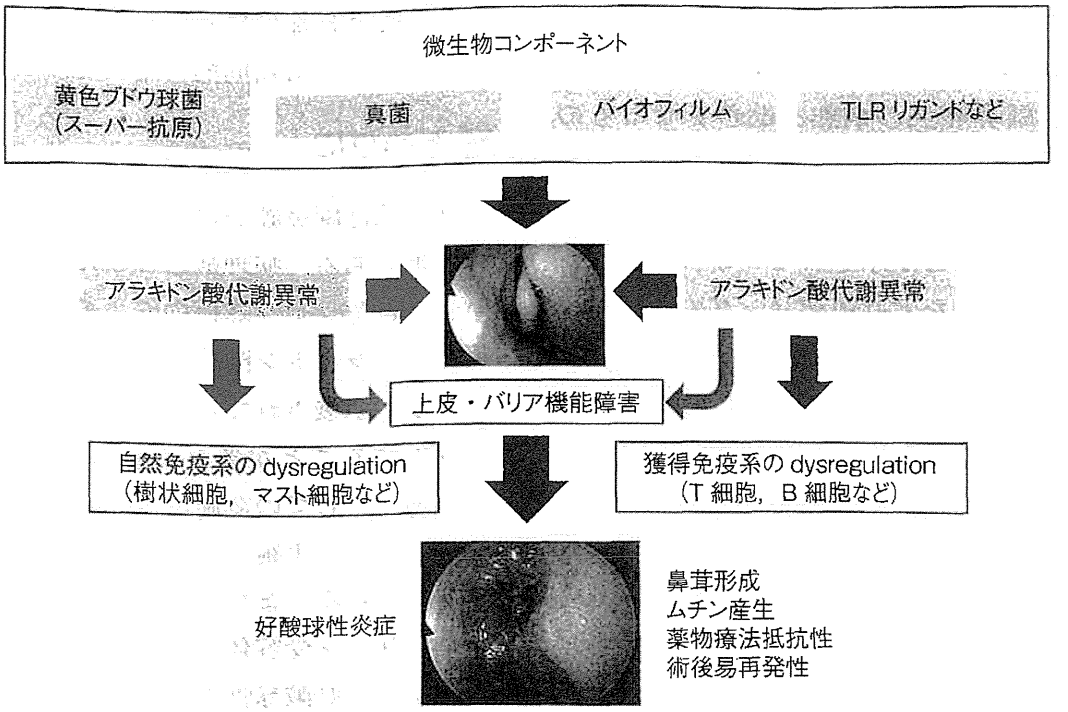

図 2　好酸球性副鼻腔炎の難治化要因

(LPS) は Toll 様受容体 (TLR) のリガンドの 1 つとして自然免疫系に関わる重要な分子であり，好酸球性炎症の制御にも関与する．鼻茸においては，PGE_2 は LPS による好酸球性炎症の誘導に抑制的に働く[8]．

III 好酸球性副鼻腔炎の診断

確定診断は，前述の臨床徴候に加え，鼻茸中に著明な好酸球浸潤を認めることである．しかしながら，診断のために鼻茸の生検を行うことは実際的でない．以前より鼻茸中の好酸球数と血中好酸球数が有意な正の相関を示すことが知られている．また，血中好酸球数の高値は副鼻腔手術後の再燃因子となる[9]．そこで鼻茸中好酸球数に代わり血中好酸球数を利用した，より非侵襲的で実地臨床に即した診断基準の作成が試みられている．たとえば，鼻茸を合併した副鼻腔炎のうち末梢血好酸球比率が 6% 以上かつ後部篩骨洞および嗅裂部に陰影を認める場合，好酸球性副鼻腔炎は感度 84.6%，特異度 92.3% で診断される[10]．

表 2　好酸球性副鼻腔炎に対する治療法

増悪時療法 (Reliever)	長期管理療法 (Controller)
• 経口ステロイド薬 • 抗菌薬 • 手術療法	• ロイコトリエン受容体拮抗薬 • 鼻噴霧用ステロイド薬 • Th2 サイトカイン阻害薬 • PGD_2・TXA_2 受容体拮抗薬 • マクロライド療法 • 粘液修復薬 • 局所処置 • 鼻・副鼻腔洗浄 (• 抗 IgE 抗体療法)

IV 好酸球性副鼻腔炎の治療

前述のように好酸球性副鼻腔炎の病態は喘息と類似しており，喘息に対する治療方針，すなわち reliever（レリーバー：増悪時療法）と controller（コントローラー：長期管理療法）による加療を参考にすることができる（表 2）．レリーバー，すなわち急性増悪に対する治療としては，好酸球性炎症の増悪に対する全身（経口を含む）ステロイド療法，感染に対する抗菌薬療法などが挙げられる．全身ステロイド薬の使

用については議論の余地がある．最近の二重盲検試験では，20日間の経口ステロイド薬の内服は早期に副鼻腔炎の病態を改善させるものの，3か月後ではベースラインに戻り，血中好酸球数など一部のパラメータに関してはリバウンドがみられることが示されている[11]．

また，鼻茸形成などリモデリングの進んだ状態に対してはESSが選択される．前述のように，喘息合併の副鼻腔炎患者ではESSにより尿中ロイコトリエン濃度が有意に減弱することから，one airway，one diseaseの観点からもESSが推奨される．

一方，コントローラーとしては好酸球性炎症を抑え，その結果として鼻閉やムチン産生などを改善する治療である．炎症の増悪因子となりうる細菌や真菌，あるいは炎症細胞や粘膜構築細胞から産生されたサイトカインやロイコトリエンなどの起炎性物質を除去する鼻処置や鼻・副鼻腔洗浄が基本となる．この点からも手術にて副鼻腔を大きく開放し，単洞化することが望ましい．通常はエネマシリンジや市販の鼻洗浄器を利用し，加温した生理的食塩水にて洗浄する．バイオフィルムに対してベビーシャンプーなどの界面活性剤を添加したり，抗菌作用を期待してマヌカハニー（蜂蜜）を添加する試みもある．

薬物療法としては，鼻噴霧用ステロイド薬やロイコトリエン受容体拮抗薬，PGD_2・TXA_2受容体拮抗薬，Th2サイトカイン阻害薬などの効果が知られている[12]．ステロイド薬は鼻茸においても制御性T細胞を誘導することが可能であり，この点からもコントローラーとして炎症局所に用いることが望ましい．最近では，鼻茸中にIgEが認められることを背景に，抗IgE抗体（オマリズマブ）の好酸球性副鼻腔炎に対する有効性を示す報告が集積されつつある[13]．また，14員環マクロライド系抗菌薬や粘液修復薬（カルボシステインなど）は好酸球性炎症に対して著効しないが，粘液分泌抑制などを介して副鼻腔の慢性炎症には効果があり，好酸球性副鼻腔炎に対しても補助的に用いることもある．

おわりに

好酸球性副鼻腔炎は難治性副鼻腔炎の代表的な疾患である．病理病態はまだ解明されていないが，黄色ブドウ球菌の外毒素などの外的な因子と，アラキドン酸代謝異常などの内的な因子の関与が示唆されている．また重症例では喘息を合併することが多く，“asthma of the upper airway”としての認識が必要である．増悪時療法としては，手術，経口ステロイド薬，抗菌薬が考慮される．また長期管理療法としては，ロイコトリエン受容体拮抗薬，鼻噴霧用ステロイド薬などの好酸球性炎症と抑える薬物療法と共に，局所処置や鼻・副鼻腔洗浄による微生物や炎症産物のクリアランスが重要である．

文　献

1) 森山　寛：日本耳鼻咽喉科学会専門医通信 2002；70：8-9.
2) Hamilos DL, *et al*（eds）：*Chronic rhinosinusitis : pathogenesis and medical management*. Informa Healthcare, New York, 2007；163-175.
3) Okano M, *et al*：*J Allergy Clin Immunol* 2009；123：868-874.
4) Hamilos DL, *et al*（eds）：*Chronic rhinosinusitis : pathogenesis and medical management*. Informa Healthcare, New York, 2007；177-184.
5) Okano M, *et al*：*Clin Exp Allergy* 2011；41：171-178.
6) Higashi N, *et al*：*J Allergy Clin Immunol* 2004；113：277-283.
7) Picado C, *et al*：*Am J Respir Crit Care Med* 1999；160：291-296.
8) Higaki T, *et al*：*Clin Exp Allergy* 2012；42：1217-1226.
9) Matsuwaki Y, *et al*：*Int Arch Allergy Immunol* 2008；146(Suppl 1)：77-81.
10) Sakuma Y, *et al*：*Auris Nasus Larynx* 2011；38：583-588.
11) Van Zele T, *et al*：*J Allergy Clin Immunol* 2010；125：1069-1076.
12) 岡野光博：アレルギー 2004；53：1-7.
13) Grundmann SA, *et al*：*J Allergy Clin Immunol* 2008；121：257-258.

Auris Nasus Larynx 40 (2013) 548–553

Contents lists available at SciVerse ScienceDirect

Auris Nasus Larynx

journal homepage: www.elsevier.com/locate/anl

A modified Lund–Mackay system for radiological evaluation of chronic rhinosinusitis

Tetsushi Okushi *, Tsuguhisa Nakayama, Shigemitsu Morimoto, Chiaki Arai, Kazuhiro Omura, Daiya Asaka, Yoshinori Matsuwaki, Mamoru Yoshikawa, Hiroshi Moriyama, Nobuyoshi Otori

Department of Otorhinolaryngology, Jikei University School of Medicine, Japan

ARTICLE INFO

Article history:
Received 20 August 2012
Accepted 25 April 2013
Available online 14 June 2013

Keywords:
Chronic rhinosinusitis
Computed tomography
Staging system
Lund–Mackay system
Zinreich system
Gradation
Accuracy
Visual score
Objective score
Soft tissue density rate

ABSTRACT

Objective: The Lund–Mackay system (L–M system) is widely used for computed tomography (CT) evaluation of chronic rhinosinusitis (CRS). However, a major drawback of the L–M system is its insufficiency of gradation. To avoid this deficiency, a new staging system proposed by American societies and the Zinreich system were reported as modifications of the L–M system. The aim of this study was to investigate the efficiency of gradation and the accuracy of the visual quantification of these modified staging systems.

Methods: Preoperative CT scanning was performed on 20 adult patients with CRS. A computer workstation was used to measure the volume of each sinus and the volume of inflammatory disease in each sinus. Then the soft tissue density rate (STDR) and objective scores, which were adapted to each system, were calculated. Visual evaluation of the CT images was performed using these systems. The visual score with each staging system and STDR value were evaluated for a correlation, and the rate of agreement was determined between the visual and objective scores obtained with each staging system.

Results: The correlation between the visual scores and the STDR values was shown with all staging system including L–M system. The coefficients of correlation between the visual scores and the STDR values with these modified systems were higher than with the L–M system. While the agreement rates with these modified systems were significantly lower than with the L–M system, differences of 2 or greater between the subjective and objective scores were rare.

Conclusion: We cannot conclude that one of these three staging systems is superior to the other. With this study, the simple grading system such L–M staging score was considered easy and accurate method to use the clinical level. The modified staging systems showed more efficient ability to gradate in evaluating rhinosinusitis inflammation compared with the L–M system and also showed acceptable accuracy.

1. Introduction

Computed tomography (CT) is being used to assess the volume of inflammatory load within the paranasal sinuses in chronic rhinosinusitis (CRS) and also as an aid in diagnosing and deciding the treatment of CRS [1–3]. CT is also a useful tool for objectively evaluating the degree of improvement in CRS before and after drug therapy or surgery [2].

The Lund–Mackay system [4] (L–M system) is widely used for CT evaluation of CRS. The familiarity of L–M system is owing to its simple staging (Table 1). When rhinosinusitis inflammation occupies 0% of the CT image, a score of 0 is assigned, while a score of 2 is assigned when the inflammation occupies 100% of the image. All other degrees of inflammation are scored as 1. However, it is often pointed out that this system seems to lack sufficient levels of gradation for tracking progression or reduction of the disease volume [5]. Two more detailed staging systems have been reported in recent years as modifications of the L–M system, aimed at resolving those deficiencies.

One is a staging system proposed by an expert panel formed by five American societies [5]: The American Academy of Allergy, Asthma and Immunology; The American Academy of Otolaryngic Allergy; The American Academy of Otolaryngology Head and Neck Surgery; The American College of Allergy, Asthma and Immunology; and the American Rhinologic Society. This proposed rhinosinusitis staging system (Proposed system) is shown in Table 2. It

* Corresponding author at: Department of Otorhinolaryngology, Jikei University School of Medicine, 3-25-8 Nishishinbashi, Minato-ku, Tokyo 105-8461, Japan. Tel.: +81 3 3433 1111x3601.
E-mail address: t-okushi@jikei.ac.jp (T. Okushi).

0385-8146/$ – see front matter © 2013 Elsevier Ireland Ltd. All rights reserved.
http://dx.doi.org/10.1016/j.anl.2013.04.010

Table 1
Lund–Mackey system.

Sinus	Right sinus	Left sinus
Frontal	0–2	0–2
Anterior ethmoids	0–2	0–2
Posterior ethmoids	0–2	0–2
Maxillary	0–2	0–2
Sphenoid	0–2	0–2
Ostiomeatal complex	0 or 2	0 or 2

For the sinuses: 0 = no inflammation; 1 = partial inflammation; 2 = 100% inflammation.
For the ostiomeatal complex: 0 = not occluded; 2 = occluded.
Maximum total score: 24.

Table 3
Zinreich system.

Sinus	Right sinus	Left sinus
Frontal	0–5	0–5
Anterior ethmoids	0–5	0–5
Posterior ethmoids	0–5	0–5
Maxillary	0–5	0–5
Sphenoid	0–5	0–5

For the sinuses: 0 = 0% inflammation; 1 = 1–25% inflammation; 2 = 26–50% inflammation; 3 = 51–75% inflammation; 4 = 76–99% inflammation; 5 = 100% inflammation.
Maximum total score: 50.

classifies the volume of inflammatory disease in each sinus into four strata using intervals of 33% and evaluates the inflammation score using a 4-point system.

The second staging system is the Zinreich system, shown in Table 3 [6]. This system divides the rhinosinusitis inflammation on CT images into four strata using intervals of 25% and evaluates the inflammation score using a 5-point system. The Zinreich system does not evaluate the ostiomeatal complex (OMC).

Although these modifications of the L–M staging system have the possibility to present more sufficient level of inflammatory gradation compared with the L–M system, there were few reports evaluating the actual advantage of these systems. Furthermore, in clinical practice, most of ENT doctors evaluate the inflammatory volume visually using these systems. As a result, it can be thought that the evaluation of the accuracy of the visual quantification with these systems is needed. We thus compared the efficiency of gradation and the accuracy of the visual quantification of these staging systems with the L–M system.

2. Subjects and methods

2.1. Subjects

Between April 2007 and March 2008, 552 patients who underwent endoscopic sinus surgery (ESS) for CRS in the Department of Otorhinolaryngology of the Jikei University School of Medicine satisfied the inclusion/exclusion criteria described below. For inclusion, a patient had to be an adult with CRS who underwent ESS based on the criteria reported by Meltzer et al. [5] CRS was diagnosed on the basis of the symptoms, endoscopic findings, CT imaging and allergy test results. Surgery was indicated for patients who did not respond to 3 or more months of conservative treatment.

The exclusion criteria consisted of unilateral CRS, presence of a sinus defect, a history of sinus surgery, presence of a systemic disease that would affect the nose, presence of a sinus bone lesion (e.g., Wegener's granulomatosis, cystic fibrosis, Kartagener's syndrome, sarcoidosis, etc.) and a history of facial trauma.

Table 2
Proposed system.

Sinus	Right sinus	Left sinus
Frontal	0–4	0–4
Anterior ethmoids	0–4	0–4
Posterior ethmoids	0–4	0–4
Maxillary	0–4	0–4
Sphenoid	0–4	0–4
Ostiomeatal complex	0 or 2	0 or 2

For the sinuses: 0 = 0% inflammation; 1 = 1–33% inflammation; 2 = 34–66% inflammation; 3 = 67–99% inflammation; 4 = 100% inflammation.
For the OMC: 0 = not occluded; 2 = occluded.
Maximum total score: 44.

For the present study, twenty patients (40 nasal sides) were selected from the 552 patients. To prevent imbalance in the severity of inflammatory disease, 552 patients were divided into four strata based on L–M staging score except for OMC score using intervals of 5 (strata 1: L–M staging score = 0–5, strata 2: L–M staging score = 6–10, strata 3: L–M staging score = 11–15, strata 4: L–M staging score = 16–20). L–M staging score was referred from clinical records. Each number of four strata was 154 in strata1, 228 in strata 2, 112 in strata 3, 58 in strata4, respectively. A random sample from each stratum was taken in a number proportional to the stratum's size (6 samples from strata1, 8 samples from strata 2, 4 samples from strata 3, 2 samples from strata 4). The study was approved by the Ethics Committee of Jikei University School of Medicine.

Because the OMC is not included in the evaluations performed by the Zinreich system, the OMC was also not evaluated by the L–M system or the Proposed system in this study. Therefore, in this study, the maximum possible total score was 20 with the L–M system and 40 with the Proposed system.

2.2. Soft tissue density rate

To quantify the volume of inflammatory opacification, the soft tissue density rate (STDR; %) was assessed with a computer workstation. Axial images were acquired preoperatively with Multi-slice CT helical scanning using a Siemens SOMATOM Sensation 16 (Siemens, Berlin, Germany) (parameters: 120 kV, 500 mA, and 2-s scan time). A computer workstation (Synapse ver. 3.1.1; Fujifilm Medical Systems, CT, USA) was used to measure the area of each nasal sinus and the area of soft tissue density for each slice in the CT axial sections of the patients (Fig. 1). Then the approximate values for the volume of each sinus and the volume of soft tissue density in each sinus were calculated by adding the respective areas for each slice and multiplying by the slice width. The CT axial section slice width ranged from 3 to 5 mm, with a mean of 4.1 mm. STDR was calculated by dividing the volume of soft tissue density in each sinus by the volume of each sinus (STDR = volume of soft tissue density in each sinus/volume of each sinus × 100%).

2.3. Objective score

To evaluate the exact scores for each sinus, the STDR value for each sinus was compared with the scores assigned in accordance with the L–M system, the Proposed system and the Zinreich system, and then the objective scores generated with each staging system were calculated for each sinus (example: STDR = 61% → L–M score = 1, Proposed score = 2, Zinreich score = 3).

2.4. Visual score

Three rhinologists, specializing in sinus diseases and having undergone training in evaluation of the volume of soft tissue

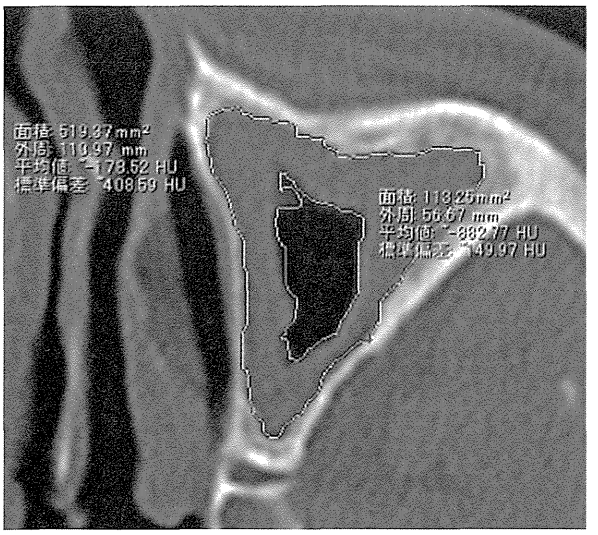

Fig. 1. Assessment of soft tissue density rate. The area of each nasal sinus and the area of soft tissue density were measured for each slice in the preoperative CT horizontal sections. Then the approximate values for the volume of each sinus and the volume of soft tissue density in each sinus were calculated by adding the respective areas for each slice and multiplying by the slice width. STDR was calculated by dividing the volume of inflammatory disease in each sinus by the volume of each sinus (STDR = volume of soft tissue density in each sinus/volume of each sinus ×100%).

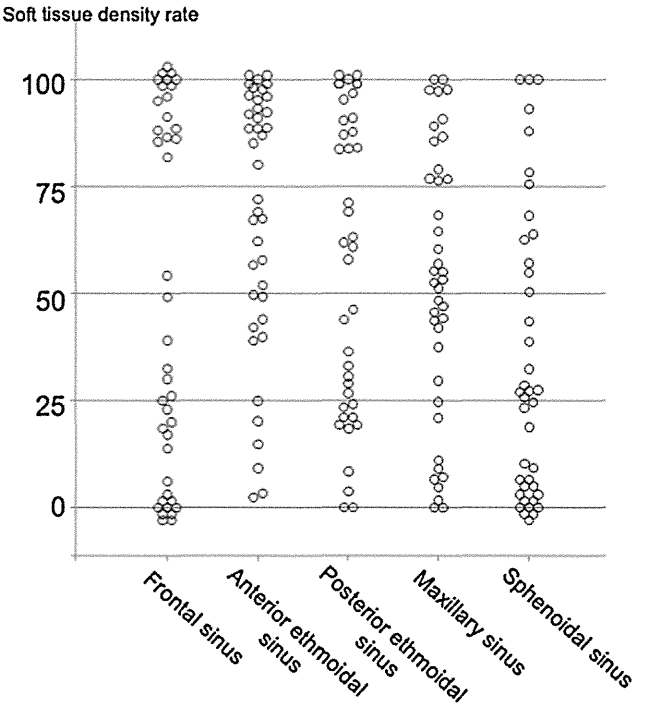

Fig. 2. Distribution of STDR in each sinus. For the frontal sinus, there were no data in the vicinity of STDR = 75%. For the anterior ethmoid sinus, the most common STDR was ≥50%. For the other sinuses, the STDR values were distributed nearly evenly from 0% through 100%.

density by CT scanning, independently performed visual evaluation of the CT images for each of the 20 patients in a blind fashion by application of the L–M system, the Proposed system and the Zinreich system.

2.5. Data analysis

The visual scores were compared with the STDR values and objective scores. The visual score and STDR value with each staging system were evaluated for a correlation using Pearson's correlation coefficient. Then the rate of agreement was determined between the visual score and objective score obtained with each staging system.

In addition, each sinus whose visual and objective scores were not in accord was investigated regarding its location and the extent of disagreement.

3. Results

3.1. Distribution of STDR in each sinus

Fig. 2 shows the STDR values for each sinus that were generated from the CT images for the 40 nasal sides of the 20 patients. For the frontal sinuses, there were no data in the vicinity of STDR = 75%, whereas the 0% and 100% groups were predominant. For the anterior ethmoids, the most common STDR was ≥50%, while there were no STDR = 0% cases. For the other sinuses, the STDR values were distributed nearly evenly from 0% through 100%.

3.2. Correlations between visual scores and STDR values and agreement rates between the visual and objective scores with each staging system

Fig. 3 shows the data for the coefficients of correlation between the visual scores and the STDR values with each of the three staging systems. The coefficient of correlation between the visual scores and the STDR values with the L–M system was 0.699 ($P < 0.001$). With the Proposed system and the Zinreich system, the respective coefficients of correlation were 0.883 ($P < 0.001$) and 0.917 ($P < 0.001$), which were higher than with the L–M system. Inflammatory gradations with modified L–M system seemed sufficient level to some extent.

The P values and the rates of agreement between the objective and visual scores with each of the three staging systems were shown in Table 4. The agreement rate data was the mean rates for the 3 physicians who performed the evaluations, together with the lowest and highest values.

The mean agreement rate between the objective and visual scores with the L–M system was 97.0% (96.5–97.5%). The mean rates with the Proposed and Zinreich systems were significantly lower than with the L–M system: 74.3% (73.5–74.5%) and 70.5% (66.5–73.0%), respectively ($P < 0.01$). The difference between the Proposed and Zinreich systems was not statistically significant ($P = 0.27$).

Fig. 4 shows the data for the percent and extent of disagreement between the visual and objective scores with each staging system. The percentage of the total nasal sides that showed a [visual score − objective score] of ±1 was 3.0% with the L–M system, 23.7% with the Proposed system and 24.0% with the Zinreich system. Similarly, the percentage of the total nasal sides that showed a [visual score–objective score] of ≥2 or ≤−2 was 2.0% with the Proposed system and 5.5% with the Zinreich system. With the L–M system, there were no cases of a [visual score − objective score] of ≥2.

3.3. The incidences of disagreement between the subjective and objective scores for each sinus

Fig. 5 presents the results for the incidences of disagreement between the visual and objective scores for each sinus with each staging system. With the L–M system, more than 80% of the cases of disagreement occurred in the ethmoids. The percentages were almost the same for the anterior and posterior ethmoids. In comparison, the incidences were lower for the frontal and

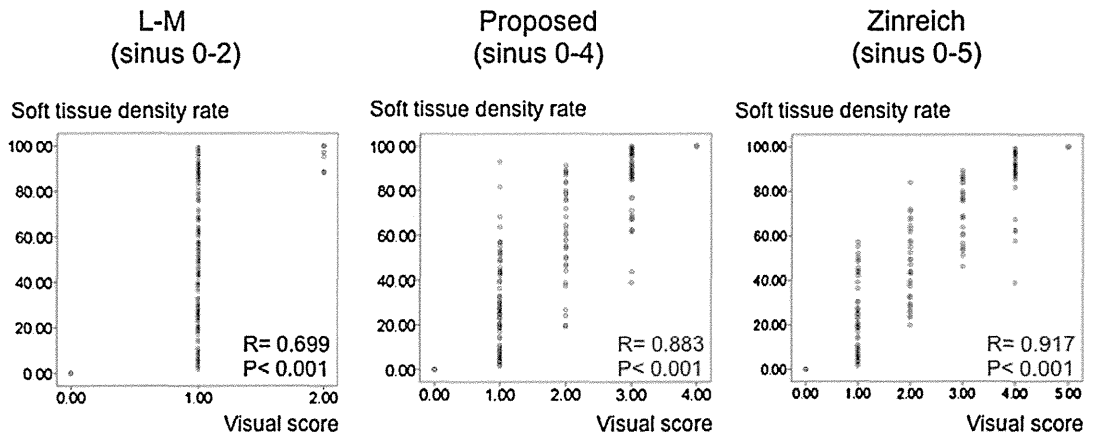

Fig. 3. Correlations between visual score and STDR values with each staging system. Each visual score in this figure represented independent score of three authorized rhinologists. The coefficient of correlation between the visual scores and the STDR values with the L–M system was 0.699 ($P < 0.001$). With the Proposed system and the Zinreich system, the respective coefficients of correlation were 0.883 ($P < 0.001$) and 0.917 ($P < 0.001$), which were higher than with the L–M system.

maxillary sinuses, while no cases of disagreement were observed for the sphenoids. With the Proposed and Zinreich systems, the incidences of disagreement between the visual and objective scores were in the range of 20–30% for the anterior/posterior ethmoids and the maxillary sinuses. The percentage was lowest for the frontal sinuses, followed by the sphenoids.

4. Discussion

CT plays two main roles in regard to CRS. One is to elucidate the anatomy of the nasal sinuses prior to ESS, thereby providing the surgeon information that will enable a safe and sufficient approach to the sinuses. The second is to assess the extent and severity of lesions in CRS and aid in diagnosing and deciding the treatment of the disease [7].

Recent years have seen various attempts to classify the stages of inflammatory disease in the sinuses of CRS patients based on the CT image findings [2,4,6,8]. The staging system most commonly applied around the world is the L–M system [4], and it is extensively used to evaluate the extent and prognosis of lesions in the sinuses [9–13]. However, the L–M system is suggested to include its insufficient levels of gradation for tracking progression or reduction of the disease volume [5,8]. With the aim of resolving this issue, more detailed staging systems have been developed by modifying the L–M system [5,6]. The modified staging systems aim at more refined evaluation and classification of the extent of sinus inflammation between 0% and 100% compared with the L–M system.

In clinical practice, most of ENT doctors perform visual evaluation of the inflammatory volume using these systems. Deeb et al. attempted the three-dimensional volumetric measurements of the maxillary sinus using an image analysis software [14]. This measurement represent a new and unique way to evaluate CT scans in patients with CRS. However, this method is too cumbersome to evaluate the whole sinus in a large number of patients. So it can be surmised that a disparity may manifest between the actual extent of inflammation and the visual extent assessed with a more detailed or refined staging system. To date, this issue has not been addressed, which was the impetus for our present study comparing the modified staging systems' efficient levels of gradation and their accuracy in visual evaluating rhinosinusitis inflammation relative to the L–M system.

Table 4
Agreement rates between the visual and objective scores with each staging system.

	Mean agreement rate VS/OS (lowest-highest) %	
Lund-Mackey system	97.0 (96.5-97.5)	*
Proposal system	74.3 (73.5-74.5)	*
Zinreich system	70.5 (66.5-73.0)	

VS: visual score; OS: objective score.
*$P < 0.01$ Mann–Whitney U test.

In this study, the correlation between the visual scores and the STDR values was shown with all staging system including L–M system. The coefficient of correlation between the visual score and the STDR value was stronger with the Proposed system and the Zinreich system than with the conventional L–M system. However, the rate of agreement between the visual and objective scores was significantly lower with the Proposed and the Zinreich systems than with the L–M system. Thus, our results were conflicting: the modified staging systems' ability to subgrade rhinosinusitis inflammation was increased, whereas their rate of visual/objective score agreement was decreased. For that reason, we cannot conclude that one of these three staging systems is superior to the other.

With the Proposed system and the Zinreich system, a [visual score – objective score] of ±1 was seen at respective rates of 23.7% and 24.0%. While a value of ±1 can be tolerated in objective evaluations of sinus inflammation, differences of 2 or greater between the visual and objective scores were observed at rates of only 2.0% and 5.5% with the Proposed system and the Zinreich system, respectively. As a result, it can be thought that clinical application of the Proposed and Zinreich systems is feasible. No great differences were found between the Proposed and Zinreich systems in terms of their efficient levels of gradation or their accuracy.

The rate of disagreement between the visual and objective scores was lowest for the frontal sinuses and sphenoids with each staging system. The rates were about the same for the anterior and posterior ethmoids with the L–M staging system, and for the anterior and posterior ethmoids and the maxillary sinuses with the Proposed and Zinreich systems. The three physicians who independently evaluated the inflammation in each nasal sinus on the basis of the CT image findings used mainly coronal sections for the classification. When they used coronal sections to evaluate the frontal sinuses, the average number of coronal slices to be checked was 5.4. Conversely, when they evaluated the anterior/posterior ethmoids, sphenoids and maxillary sinuses using coronal sections,

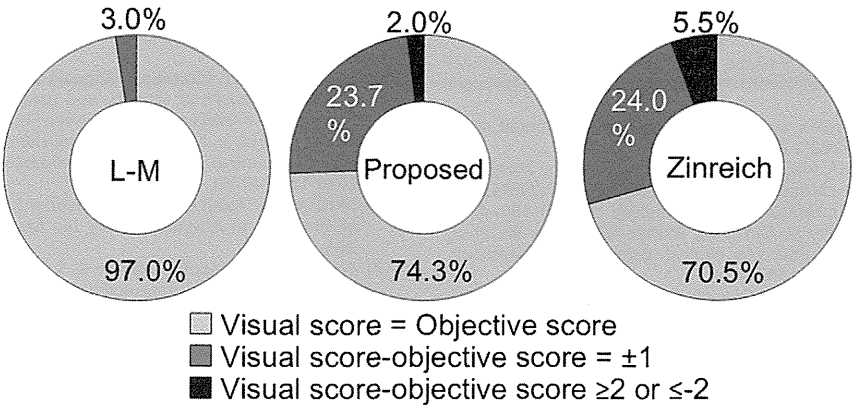

Fig. 4. The incidences of agreement and disagreement between the subjective and objective scores with each staging system. The percentage of the total nasal sides that showed a [subjective score – objective score] of ±1 was 3.0% with the L–M system, 23.7% with the Proposed system and 24.0% with the Zinreich system. The percentage of the total nasal sides that showed a [subjective score – objective score] of ≥2 or ≤−2 was 2.0% with the Proposed system and 5.5% with the Zinreich system.

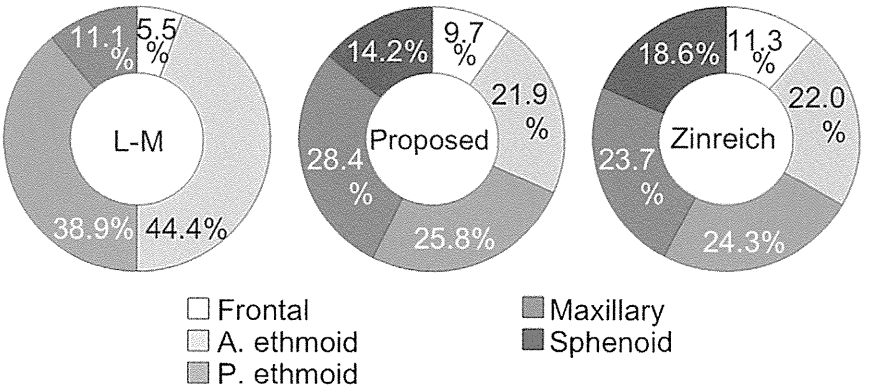

Fig. 5. The incidences of disagreement between the subjective and objective scores for each sinus with each staging system. With the L–M system, more than 80% of the cases of disagreement occurred in the ethmoids. The percentages were low for the frontal sinus and the anterior ethmoid, and there were no cases of disagreement for the sphenoid. With the proposed and Zinreich systems, the incidences of disagreement between the subjective and objective scores were in the range of 20–30% for the anterior/posterior ethmoids and the maxillary sinus. The percentage was lowest for the frontal sinus, followed by the sphenoid sinus.

the average numbers of coronal slices to be checked were 8.1, 8.5 and 12.8, respectively. So it can be surmised that the evaluation of the frontal sinus was not especially complicated since the number of coronal slices was low.

The overall rate of disagreement was very low with the L–M system, but it was high for the anterior and posterior ethmoids. The ethmoids have complex anatomical structures, and there are cases when it is difficult to distinguish the anterior and posterior ethmoids on CT images. This can be thought to be the cause of the high rates of disagreement for these sinuses with the L–M system.

There are two concerns, which have possibility to affect the outcome of this study. One is the small sample size, and another is incomplete distribution of STDR. The STDR values for each sinus that were generated from the CT images for the 40 nasal sides of 20 patients showed slight bias in the frontal sinuses and the anterior ethmoids. For the other sinuses, the distribution of STDR values was nearly uniform from 0% to 100%. There were few patients with CRS who showed no inflammation in the ethmoid sinuses, and it may be difficult to eliminate the bias seen for the anterior ethmoids. Considering such difficulty, we performed the present study to investigate the Proposed and Zinreich systems – which are modifications of the L–M system – for their sufficient levels of gradation and accuracy in evaluating rhinosinusitis inflammation. Our findings show that these systems are successful in achieving a certain level of evaluation.

In this study, relationship between CT staging and clinical symptoms was not investigated. Zheng et al. reported the significant but weak correlation between L–M system and clinical symptoms [15]. Additional study of the correlations between clinical symptoms and these modifications of the L–M system are needed.

5. Conclusion

With this study, consequently, the simple grading system such L–M staging score was considered easy and accurate method to use the clinical level. The Proposed system and the Zinreich system showed more efficient ability to gradate in evaluating rhinosinusitis inflammation compared with the L–M system. If a value of ±1 for [visual score – objective score] can be tolerated, then it can be thought that the Proposed and Zinreich systems show acceptable accuracy. No great differences were found between the Proposed and Zinreich systems in terms of their sufficient levels of gradation or their accuracy. It is hoped that these modified staging systems will be further investigated in the clinical setting and their appropriateness will be examined in various studies.

Conflicts of interest

None.

References

[1] Lloyd GA, Lund VJ, Scadding GK. CT of the paranasal sinuses and functional endoscopic surgery: a critical analysis of 100 symptomatic patients. J Laryngol Otol 1991;105:181–5.

[2] Kennedy DW. Prognostic factors, outcomes and staging in ethmoid sinus surgery. Laryngoscope 1992;102:1–18.

[3] Young J, Frenkiel S, Tewfik MA, Mouadeb DA. Long-term outcome analysis of endoscopic sinus surgery for chronic sinusitis. Am J Rhinol 2007;21:743–7.

[4] Lund VJ, Mackay IS. Staging in rhinosinusitus. Rhinology 1993;31:183–4.

[5] Meltzer EO, Hamilos DL, Hadley JA, Lanza DC, Marple BF, Nicklas RA, et al. Rhinosinusitis: establishing definitions for clinical research and patient care. J Allergy Clin Immunol 2004;114:155–212.

[6] Kennedy DW, Kuhn FA, Hamilos DL, Zinreich SJ, Bulter D, Warsi G, et al. Treatment of chronic rhinosinusitis with high-dose oral terbinafine: a double blind, placebo-controlled study. Laryngoscope 2005;115:1793–9.

[7] Bhattacharyya N. Clinical and symptom criteria for the accurate diagnosis of chronic rhinosinusitis. Laryngoscope 2006;116:1–22.

[8] Metson R, Gliklich RE, Stankiewicz JA, Kennedy DW, Duncavage JA, Hoffman SR, et al. Comparison of sinus computed tomography staging systems. Otolaryngol Head Neck Surg 1997;117:372–9.

[9] Friedman WH, Katsantonis GP, Bumpous JM. Staging of chronic hyperplastic rhinosinusitis: treatment strategies. Otolaryngol Head Neck Surg 1995; 112:210–4.

[10] Bhattacharyya T, Piccirillo J, Wippold 2nd FJ. Relationship between patient-based descriptions of sinusitis and paranasal sinus computed tomographic findings. Arch Otolaryngol Head Neck Surg 1997;123:1189–92.

[11] Bhattacharyya N, Lee LN. Evaluating the diagnosis of chronic rhinosinusitis based on clinical guidelines and endoscopy. Otolaryngol Head Neck Surg 2010;143:147–51.

[12] Mortuaire G, Bahij J, Maetz B, Chevalier D. Lund–Mackay score is predictive of bleeding in ethmoidectomy for nasal polyposis. Rhinology 2008;46: 285–8.

[13] Poetker DM, Mendolia-Loffredo S, Smith TL. Outcomes of endoscopic sinus surgery for chronic rhinosinusitis associated with sinonasal polyposis. Am J Rhinol 2007;21:84–8.

[14] Deeb R, Malani PN, Gill B, Jafari-Khouzani K, Soltanian-Zadeh H, Zacharek MA, et al. Three-dimensional volumetric measurements and analysis of the maxillary sinus. Am J Rhinol 2011;25:152–6.

[15] Zheng Y, Zhao Y, Lv D, Liu Y, Qiao X, Wang D, et al. Correlation between computed tomography staging and quality of life instruments in patients with chronic rhinosinusitis. Am J Rhinol 2010;24:e41–5.

Allergology International. 2013;62:495-502
DOI: 10.2332/allergolint.13-OA-0572

ORIGINAL ARTICLE

Increased CXCL10 Expression in Nasal Fibroblasts from Patients with Refractory Chronic Rhinosinusitis and Asthma

Mamoru Yoshikawa[1], Kota Wada[2], Tsuyoshi Yoshimura[2], Daiya Asaka[2], Naoko Okada[3], Kenji Matsumoto[3] and Hiroshi Moriyama[2]

ABSTRACT

Background: Chronic rhinosinusitis (CRS) is characterized by local inflammation of the sinonasal tissues. CRS patients with nasal polyps and asthma often develop acute exacerbation of sinonasal symptoms after upper respiratory tract infections. However, the influence of concomitant asthma on the nasal immune response to viral infection remains unclear.

Methods: Specimens of nasal polyp and mucosal tissues were obtained from 3 groups of CRS patients (n = 14 per group): 1) patients without asthma (CRS group), 2) patients with aspirin-tolerant asthma (ATA group), and 3) patients with aspirin-intolerant asthma (AIA group). Nasal fibroblasts isolated from the specimens were stimulated with poly I:C. CXCL10 expression was analyzed by the quantitative real-time polymerase chain reaction and enzyme-linked immunoadsorbent assay. Biopsy specimens from CRS patients without asthma were subjected to immunohistochemistry for detection of T-bet and GATA-3 expression in CD3+ T cells by double labeling.

Results: Nasal fibroblasts from the ATA and AIA groups showed significantly enhanced expression of CXCL 10 mRNA and protein after poly I:C stimulation compared with cells from the CRS group and the control group (normal nasal mucosa). In addition to T helper (Th)2 cells, there was more abundant infiltration of Th1 cells into tissues from the AIA and ATA groups.

Conclusions: Our findings suggest that CRS associated with asthma may become intractable through the over-production of CXCL10 in response to viral infection.

KEY WORDS

asthma, CXCL10 chemokine, fibroblast, nasal polyps, rhinosinusitis

INTRODUCTION

Chronic rhinosinusitis (CRS) is a common chronic disease worldwide that is treated with medication (e.g., corticosteroids[1] or macrolides[2]) and by endoscopic sinus surgery.[3] Although there has been a recent increase in the cure of CRS following the introduction of these treatments,[4,5] a substantial number of patients still have a poor outcome. In CRS patients, nasal polyps arise from the paranasal sinus mucosa and prolapse into the nasal cavity, causing persistent nasal obstruction. We have often found that CRS patients with nasal polyps and asthma show acute exacerbation of nasal symptoms after upper respiratory tract infection. It has been reported that nasal polyps and asthma are linked by shared inflammation of the entire airway mucosa, and particularly by increased infiltration of eosinophils.[6] In addition, mucosal eosinophilia is frequently associated with more severe disease and with recurrence of polyps after sur-

[1]Department of Otorhinolaryngology, Toho University School of Medicine, [2]Department of Otorhinolaryngology, Jikei University School of Medicine and [3]Department of Allergy and Immunology, National Research Institute for Child Health and Development, Tokyo, Japan.
Conflict of interest: No potential conflict of interest was disclosed.

Correspondence: Dr. Mamoru Yoshikawa, Department of Otorhinolaryngology, Toho University School of Medicine, 2-17-6 Ohashi, Meguro-ku, Tokyo 153-8515, Japan.
Email: mamoru.yoshikawa@med.toho-u.ac.jp
Received 22 April 2013. Accepted for publication 3 July 2013.

Table 1 Clinical characteristics of the four groups

	Control	CRS	ATA	AIA
No.	7	14	14	14
Sex (F/M)	1/6	2/12	4/10	7/7
Age (yr), mean	26.75 ± 9.29	44.14 ± 16.08	43.75 ± 14.42	47.17 ± 20.21
Age (yr), range	19-40	20-71	18-65	26-71
Allergic rhinitis	0 (0%)	5 (35.7%)	5 (35.7%)	2 (14.3%)
Total IgE (IU/ml)	96.5 ± 58.48	100.25 ± 142.65	257.91 ± 258.73	232.33 ± 373.03
Peripheral blood eosinophils (%)	3.03 ± 2.49	2.57 ± 1.26	8.33 ± 4.44	13.5 ± 10.82

gery.[7] Furthermore, CRS patients with aspirin-intolerant asthma often have particularly severe asthma that is associated with rhinorrhea and recurrent nasal polyps.[8,9] These findings suggest that concomitant asthma may contribute to the pathophysiology of CRS.

Rhinoviruses are the most common cause of viral upper respiratory tract infections, being responsible for up to 50% of all episodes of the common cold.[10] Viral infections have been shown to cause obstruction of the osteomeatal complex, which is thought to be a critical step in the development of CRS. Viral dsRNA and its synthetic analogue (poly I:C) are recognized by multiple pathways involving toll-like receptor 3 (TLR3), the protein kinase receptor, and two recently described genes: cytosolic RNA helicases retinoic acid-inducible gene-I (RIG-I) and melanoma differentiation-associated gene 5 (MDA5).[11] Infection of airway epithelial cells leads to release of various pro-inflammatory mediators, including interleukin (IL)-1, IL-6, IL-8, interferon-inducible protein of 10 kDa (IP-10)/CXCL10, regulated on activation normal T-cell expressed (RANTES), granulocyte macrophage-colony stimulating factor, and eotaxin.[12-14] These cytokines and chemokines recruit inflammatory cells, such as neutrophils, lymphocytes, and eosinophils, to sites of inflammation, and contribute to the exacerbation of acute and chronic inflammation.

Histologically, fibroblasts are abundant in the stroma of nasal polyps and are thought to be involved in the pathogenesis of CRS associated with polyps. Although airway epithelial cells are the main target of viral infection, several studies have detected rhinovirus in the subepithelial layer by in situ hybridization[15] and have shown that human airway fibroblasts are susceptible to rhinovirus infection.[16] In addition, it has been reported that fibroblasts produce type I interferons (IFNs) and CXCL10 after stimulation with dsRNA.[17,18] CXCL10 targets CXC chemokine receptor 3, leading to activation of natural killer cells and activated T cells, especially T helper (Th)1 cells. CXCL10 plays an important role in various Th1-dominant diseases, such as viral and bacterial infections, autoimmune diseases, and transplant rejection.[19-21] Thus, fibroblasts may also contribute to the pathogenesis of such diseases through an influence on the inflammatory response.[22] However, little is known about the response of fibroblasts to viral infection in CRS patients with nasal polyps and concomitant asthma.

In this study, we classified CRS patients with nasal polyps based on the presence or absence of asthma and investigated CXCL10 expression by nasal fibroblasts in response to stimulation by factors associated with viral infection. In addition, biopsy specimens from these patients were subjected to immunohistochemistry with double labeling to detect the expression of T-bet (the master regulator of Th1 responses) and its antagonist GATA-3 in CD3+ T cells.

METHODS

SUBJECTS

A specimen of nasal polyp mucosa was obtained during surgery from 49 patients who had been referred to Jikei University Hospital for endoscopic sinus surgery (Table 1). Specimens were obtained from 3 different groups of CRS patients: 1) 14 CRS patients who had nasal polyps without asthma (CRS group), 2) 14 patients who had polyps and aspirin-tolerant asthma (ATA) (ATA group), and 3) 14 patients with polyps and aspirin-intolerant asthma (ATA group). We excluded CRS patients without polyps because our aim was to investigate the features of polyp tissues in this disease.[23] Specimens from 7 controls were also examined (middle turbinate mucosa was obtained from 5 patients with non-allergic rhinitis and middle meatus mucosa was harvested from 2 patients with blowout fractures). Written informed consent was obtained from all of the patients prior to enrolment, and this study was approved by the Ethics Committee of Jikei University Hospital (reference number: 22-130 6307). The clinical data of the subjects are summarized in Table 1. Before endoscopic sinus surgery, each patient's serum immunoglobulin E level and peripheral eosinophil count were measured, and sinus CT scanning was performed.

CLINICAL ASSESSMENT

The diagnosis of CRS was based on typical symptoms (nasal congestion, dysosmia, etc.) documented in the medical history, the presence of endoscopically visible nasal polyps arising from the middle meatus, and

involvement of the ethmoidal and maxillary sinuses on CT scans of the paranasal sinuses. The diagnosis of asthma was made by physicians at the Department of Pulmonology of Jikei University Hospital, based on a history of typical symptoms, while AIA was diagnosed from a history of exacerbation of asthma, nasal congestion, and/or rhinorrhea after intake of aspirin or other nonsteroidal anti-inflammatory drugs.

CELL CULTURE

Nasal tissues obtained during endoscopic sinus surgery were chopped into small pieces and fibroblasts from each specimen were cultured at 37℃ in Dulbecco's modified Eagle's medium/F12 (DMEM/F12; Invitrogen, Carlsbad, CA, USA) with 10% fetal bovine serum (JRH Biosciences, Lenexa, KS, USA), 100 units/ml of penicillin, and 100 μg/ml of streptomycin (Life Technologies, Grand Island, NY, USA) under an atmosphere of 5% CO_2 and humidified air. Nasal fibroblasts were used after 3 or 4 passages.

STIMULATION OF NASAL FIBROBLASTS

Nasal fibroblasts were seeded in 6-well and 24-well culture plates (Becton-Dickinson, Franklin Lakes, NJ, USA). When the cells had reached 80% confluence, the culture medium was replaced with DMEM/F12 (Life Technologies). Then cells were stimulated with 10 μg/ml of poly I:C (Life Technologies), 10^3 units of IFN-β (PBL InterferonSource, Piscataway, NJ, USA), 10 ng/ml of IFN-γ (R&D Systems, Minneapolis, MN, USA), or 10 ng/ml of TNFα (R&D Systems) for 3 hours before extraction of mRNA and for 24 or 48 hours before harvesting the culture supernatant.

QUANTITATIVE REAL-TIME POLYMERASE CHAIN REACTION (qRT-PCR) FOR CXCL10 mRNA EXPRESSION IN NASAL FIBROBLASTS

Total RNA was isolated by using an RNeasy Mini Kit that included DNase (Qiagen, Hilden, Germany) and was transcribed to obtain cDNA by using superscript II (Life Technologies). Then the quantitative polymerase chain reaction (qRT-PCR) was performed with an ABI/PRISM 7700 Sequence Detector System (Applied Biosystems, Foster City, CA, USA) and SYBR green PCR master mix (Life Technologies). The primers were as follows: CXCL10: 5'-TGTCAGTGCT GCTACTCCACCT-3' (forward) and 5'-CTGTGTATC CAAGACAGCAGTCAA-3' (reverse), GAPDH; 5'-GAA GGTGAAGGTCGGAGTC-3' (forward) and 5'-GAAGA TGGTGATGGGATTTC-3' (reverse). The level of CXCL10 mRNA expression was normalized by the average expression of GAPDH.

ENZYME-LINKED IMMUNOSORBENT ASSAY (ELISA) FOR CXCL10 PROTEIN

Briefly, 96-well plates (Nunc, Roskilde, Denmark) were coated with 2.0 μg/ml of anti-human CXCL10 monoclonal antibody (R&D Systems) overnight at 4℃. Then the plates were washed and blocked with blocking solution (Boehringer, Mannheim, Germany). After adding a supernatant sample or standard to the wells, the plates were incubated overnight at 4℃. After washing with PBS containing 0.05% Tween 20, 100 ng/ml of biotinylated polyclonal CXCL 10 antibody was added, and the plates were incubated for 2 hours at room temperature. Further washing was done and 100 μl of streptavidin-horseradish peroxidase (Life Technologies) was added, after which the plates were let stand for 20 min at room temperature. Next, the wells were washed, and TMB (KPL, Gaithersburg, MD, USA) was added. The reaction was stopped with 2N H_2SO_4, and absorbance was measured at 450 nm with a microtiter ELISA reader (Model 550; Bio-Rad Laboratories, Hercules, CA, USA). Data were analyzed with Microplate Manager Software version 5.2.1 (Bio-Rad Laboratories), and the CXCL10 concentration in each culture supernatant was calculated from standard titration curves by linear regression analysis.

IMMUNOHISTOCHEMISTRY

Immunohistochemistry was performed with deparaffinized 4 μm sections cut from paraffin-embedded nasal tissue blocks. The paraffin-embedded sections and slides were blocked by incubation with 5% diluted normal donkey serum (Chemicon International, Temecula, CA, USA) for 30 minutes at room temperature. Then sections were incubated with primary mouse anti-T-bet polyclonal antibody (R&D Systems), mouse anti-GATA-3 polyclonal antibody (Santa Cruz Biotechnology, Santa Cruz, CA, USA), and rabbit anti-CD3 polyclonal antibody (Abcam, Cambridge, UK) overnight at 4℃. The secondary antibodies were Alexa 555-conjugated donkey anti-mouse IgG (Life Technologies) and Alexa 488-conjugated donkey anti-rabbit IgG (Life Technologies), and incubation was done for 30 minutes. After washing with PBS, sections were incubated for 5 min with 4',6-diamidino-2-phenylindole dihydrochloride (Dojindo, Kumamoto, Japan) and mounted with Permafluor (Beckman Coulter, Miami, FL, USA). Then the sections were viewed using a Biorevo BZ-9000 microscope (Keyence, Osaka, Japan).

STATISTICAL ANALYSIS

Analyses were performed using a statistical package (SPSS version 19; IBM, Armonk, NY, USA). All analyses were nonparametric. Between-group comparisons were performed by the nonparametric Mann-Whitney's *U*-test with Bonferroni correction, and differences were considered significant at $P < 0.05$.

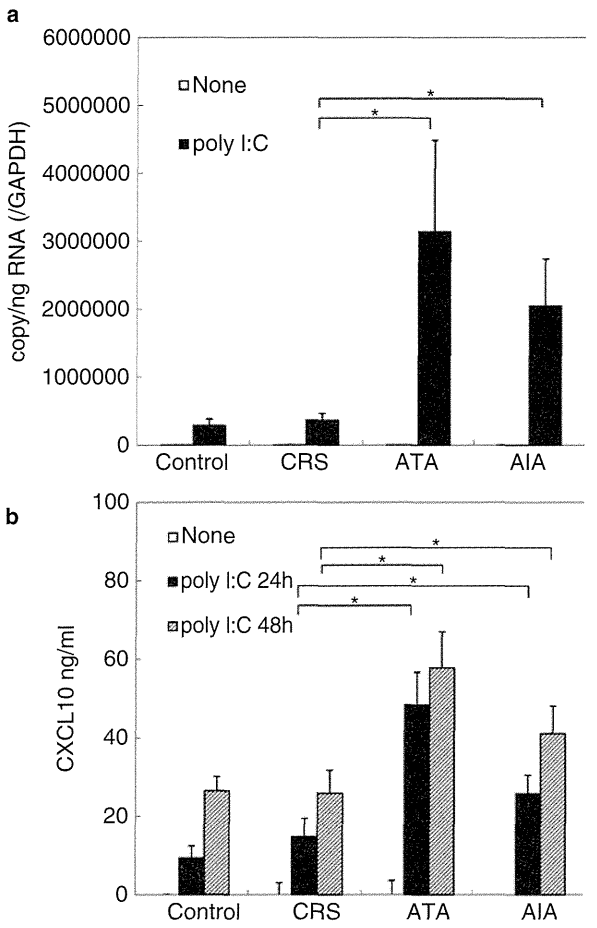

Fig. 1 *CXCL10* mRNA expression in nasal fibroblasts after poly I:C stimulation. (**a**) *CXCL10* mRNA expression in nasal fibroblasts assessed by qRT-PCR. Cultured fibroblasts were stimulated by exposure to poly I:C (10 μg/ml) for 3 hours. Copy numbers are expressed as the number of transcripts. Results were normalized by the expression of glyceraldehyde-3-phosphate dehydrogenase (GAPDH). (**b**) CXCL10 concentrations in the culture supernatant. Cultured nasal fibroblasts were stimulated by exposure to poly I: C (10 μg/ml) for 24 or 48 hours. Data are shown as the mean ± SEM. *, significant difference from medium alone ($P < 0.05$).

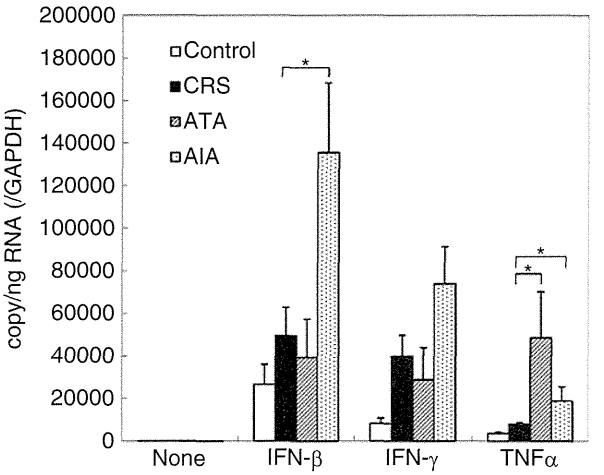

Fig. 2 *CXCL10* mRNA expression in nasal fibroblasts stimulated by cytokines. Cultured fibroblasts were stimulated by exposure to IFN-β (10^3 units), IFN-γ (10 ng/ml), or TNFα (10 ng/ml) for 3 hours. *CXCL10* mRNA expression was assessed by qRT-PCR. Data are shown as the mean ± SEM. *, significant differences from medium alone ($P < 0.05$). Copy numbers are expressed as the number of transcripts. Results were normalized by the expression of GAPDH.

RESULTS

INCREASED CXCL10 EXPRESSION IN NASAL FIBROBLASTS FROM THE AIA AND ATA GROUPS

We measured *CXCL10* mRNA expression in nasal fibroblasts from 4 groups of subjects (CRS, ATA, AIA, and control) by qRT-PCR and the results are shown in Figure 1a. In the absence of stimulation, no *CXCL 10* mRNA expression was found in any of the four groups. In response to stimulation with poly I:C (10 μg/ml), *CXCL10* mRNA expression was increased in nasal fibroblasts from all four groups. In particular, *CXCL10* mRNA expression was significantly higher in cells from the ATA group and the AIA group than in cells from the control group or the CRS group, while no significant difference was noted between the ATA and AIA groups.

We also detected CXCL10 protein in the culture supernatant of nasal fibroblasts (Fig. 1b). The concentration of CXCL10 culture supernatant from the ATA group and the AIA group was significantly higher than in supernatant from the control group or the CRS group, and the increase was time-dependent. These findings were similar to those for *CXCL10* mRNA expression.

CXCL10 mRNA EXPRESSION BY NASAL FIBROBLASTS SUBJECTED TO VARIOUS STIMULI

There are two proximal NF-κB recognition sites and the proximal interferon-stimulated response element (ISRE) within the promoter region of CXCL10.[24] After poly I:C stimulation of nasal fibroblasts, TLR-3 and RIG-I signaling activates two cellular kinases known as TANK-binding kinase-1 and IkappaB kinase-s, leading to the activation of IFN regulatory factor-3 (IRF-3) and NF-κB.[25-30] IRF-3 can also bind directly to several DNA-binding motifs, including the ISRE, leading to the direct induction of interferon-stimulated genes, such as those for IFN-α and IFN-β.[24,31,32] Therefore, we assessed *CXCL10* mRNA expression by nasal fibroblasts after stimulation with IFN-β, IFN-γ, or TNFα. As shown in Figure 2, *CXCL10* mRNA expression was induced by all three cytokines. In the control group, *CXCL10* mRNA expression was more

strongly induced by IFN-β, which activates the ISRE pathway, than by IFN-γ or TNFα. In the ATA group, *CXCL10* mRNA expression showed a significantly greater increase in response to TNFα, which activates the NF-κB pathway, than in the control group or the CRS group. On the other hand, in the AIA group, *CXCL10* mRNA expression was significantly higher than in the CRS group after stimulation with either TNFα or IFN-β.

ANALYSIS OF CELLS EXPRESSING TRANSCRIPTION FACTORS IN NASAL POLYP TISSUES

T-bet and GATA-3 are known to be the principal transcription factors involved in the differentiation of type-1 (Th1) and type-2 (Th2) helper T cells, respectively. In order to determine whether Th1 or Th2 cells were increased in nasal polyp tissues, we detected T-bet or GATA-3 and CD3 by double immunofluorescence staining. CD3+ cells were restricted to the perivascular and subepithelial regions of nasal biopsy specimens. Representative double-stained images of T-bet+CD3+ cells (Th1 cells) and GATA-3+CD3+ cells (Th2 cells) in nasal biopsy specimens are shown in Figure 3a, b. CD3+ cells were detected in all specimens, but the number of CD3+ cells was significantly higher in the ATA and AIA groups than in the control and CRS groups (Fig. 3c). In addition, the number of T-bet+CD3+ cells and GATA-3+CD3+ cells was significantly higher in the AIA group than in the control or CRS groups (Fig. 3d, e). In the ATA group, the number of T-bet+CD3+ cells and GATA-3+CD3+ cells was slightly higher than in the control group or the CRS group (Fig. 3d, e), but there were no significant differences. Thus, Th1 and Th2 cells were significantly increased in nasal polyp tissues from the AIA group compared with the control, CRS, and ATA groups.

DISCUSSION

CRS is a heterogeneous and multifactorial disease of unknown etiology. In CRS patients, inflammation of the upper and lower airways is well documented, and epidemiological and pathophysiological links between CRS with or without nasal polyps, asthma, and/or eosinophilic inflammation have been established by recent investigations. It has been shown that viral infection increases the production of a variety of proinflammatory cytokines and chemokines by epithelial cells and fibroblasts, which probably contribute to the exacerbation of airway inflammation.[33,34] In this study, we focused on the susceptibility to viral infection-related factors of fibroblasts from CRS patients with asthma (ATA and AIA). We found that the expression of *CXCL10* mRNA by nasal fibroblasts from CRS patients with asthma (ATA and AIA) was significantly upregulated in response to poly I:C compared with fibroblasts from CRS patients without asthma or controls. We also observed that both Th1 and Th2 cells were abundant in the nasal polyp tissues from CRS patients with asthma (ATA and AIA).

A previous study revealed that poly I:C significantly increases the expression of mRNAs for *CXCL10*, *CCL5*, *CXCL8*, and *IL-6* by airway epithelial cells through TLR3 signaling that is dependent on NF-κB and/or interferon regulatory factor (IRF)-3.[35] Poly I:C has also been shown to dose-dependently induce the production of CXCL10 by human fibroblasts derived from diploid skin-muscle.[36] However, this is the first report about upregulation of *CXCL10* mRNA and protein expression in nasal fibroblasts by poly I:C stimulation, and we also showed that the response was significantly greater in the ATA and AIA groups. It has been reported that fibroblasts from different individuals display distinctive characteristics that are maintained even after prolonged culture, suggesting that fibroblasts may have a highly stable imprinted phenotype.[37,38] Our results suggested that viral infection might initiate an intense inflammatory response with massive release of CXCL10 from nasal fibroblasts that are susceptible to viral infection-related factors, such as the fibroblasts isolated from the ATA and AIA groups.

We also examined the response of *CXCL10* mRNA expression to IFN-β, IFN-γ, and TNFα, in order to find key differences from poly I:C signaling, since poly I:C was reported to activate both the IRF-3 and NF-κB pathways via TLR-3 or RIG-I.[25-30] We showed that *CXCL10* mRNA expression was enhanced by TNFα in the ATA group, whereas it was significantly enhanced by both IFN-β and TNFα in the AIA group. Activation of NF-κB in nasal polyps could be important because NF-κB induces the transcription of cytokines, chemokines, and adhesion molecules that play a major role in the inflammatory process.[39] It was recently reported that IL-1β and TNF-α induce *CXCL10* mRNA expression more rapidly in asthmatic than nonasthmatic airway smooth muscle cells, with this response being mediated by the activation of NF-κB and JNK.[40] It has also been reported that TLR3 and MDA5 signaling through a common downstream intermediate (IRF3) is required for maximal sensing of rhinovirus dsRNA and is involved in CXCL10 expression.[41] More studies are needed to elucidate the role of alterations in IRF signaling.

The present study showed that Th1 and Th2 cell infiltration of nasal polyp tissues was significantly increased in the AIA group compared with the control, CRS, and ATA groups. These findings suggested that migration of Th1 cells into nasal polyps might be induced when CXCL10 is produced by fibroblasts in response to viral infection, leading to an excessive Th1-type response in CRS patients with ATA and AIA. Although there was no significant difference of Th1 and Th2 cell infiltration between the ATA group and the CRS group, CXCL10 expression was significantly

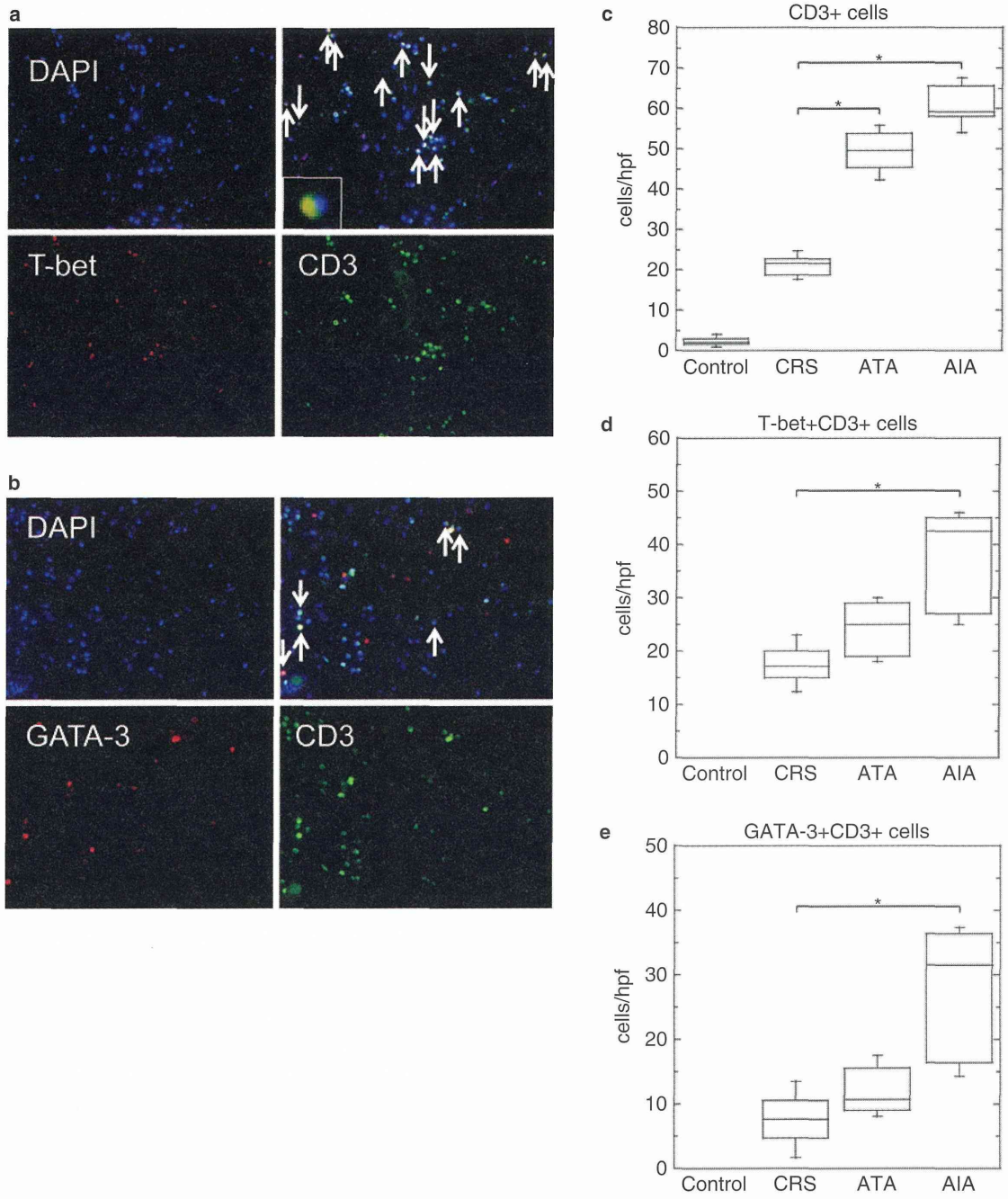

Fig. 3 Results of double immunostaining. (**a**) Representative double immunostaining of T-bet+CD3+ cells in nasal biopsy specimens. Cells were stained with DAPI (blue nuclei), CD3 (green), and T-bet (red). White arrows indicate T-bet+CD3+ cells in the merged image. Inset shows double-labeled T-bet+CD3+ cells marked by a square in the merged image. (**b**) Representative double immunostaining of GATA-3+CD3+ cells in nasal biopsy specimens. Cells were stained with DAPI (blue nuclei), CD3 (green), and GATA-3 (red). White arrows indicate GATA-3+CD3+ cells in the merged image. (**c**) CD3+ cells: The number of CD3+ cells was significantly higher in the ATA and AIA groups than in the control and CRS groups. (**d**) T-bet+CD3+ cells: The number of T-bet+CD3+ cells was significantly higher in the AIA group than in the control and CRS groups. In the ATA group, the number of T-bet+CD3+ cells was also higher than in the control and CRS groups, but the difference was not significant. (**e**) GATA-3+CD3+ cells: The number of GATA-3+CD3+ cells was significantly higher in the AIA group than in the control and CRS groups. In the ATA group, the number of GATA-3+CD3+ cells was also higher than in the control and CRS groups, but the difference was not significant.